TRPC-like conductance mediates restoration of intracellular Ca^{2+} in cochlear outer hair cells in the guinea pig and rat

Nicholas P. Raybould, Daniel J. Jagger, Refik Kanjhan, Denise Greenwood, Peter Laslo, Noriyuki Hoya, Christian Soeller, Mark B. Cannell and Gary D. Housley

Department of Physiology, University of Auckland, Private Bag 92019, Auckland, New Zealand

Ca^{2+} signalling is central to cochlear sensory hair cell physiology through its influence on sound transduction, membrane filter properties and neurotransmission. However, the mechanism for establishing Ca^{2+} homeostasis in these cells remains unresolved. Canonical transient receptor potential (TRPC) Ca^{2+} entry channels provide an important pathway for maintaining intracellular Ca^{2+} levels. TRPC3 subunit expression was detected in guinea pig and rat organ of Corti by RT-PCR, and localized to the sensory and neural poles of the inner and outer hair cells (OHCs) by confocal immunofluorescence imaging. A cation entry current with a TRPC-like phenotype was identified in guinea pig and rat OHCs by whole-cell voltage clamp. This slowly activating current was induced by the lowering of cytosolic Ca^{2+} levels ($[Ca^{2+}]_i$) following a period in nominally Ca^{2+}-free solution. Activation was dependent upon the $[Ca^{2+}]_o$ and was sustained until $[Ca^{2+}]_i$ was restored. Ca^{2+} entry was confirmed by confocal fluorescence imaging, and rapidly recruited secondary charybdotoxin- and apamin-sensitive K_{Ca} currents. Dual activation by the G protein-coupled receptor (GPCR)–phospholipase C–diacylglycerol (DAG) second messenger pathway was confirmed using the analogue 1-oleoyl-2-acetyl-*sn*-glycerol (OAG). Ion substitution experiments showed that the putative TRPC Ca^{2+} entry current was selective for $Na^+ > K^+$ with a ratio of 1 : 0.6. The Ca^{2+} entry current was inhibited by the TRPC channel blocker 2-aminoethyl diphenylborate (2APB) and the tyrosine kinase inhibitor, erbstatin analogue. We conclude that TRPC Ca^{2+} entry channels, most likely incorporating TRPC3 subunits, support cochlear hair cell Ca^{2+} homeostasis and GPCR signalling.

(Resubmitted 16 October 2006; accepted after revision 30 November 2006; first published online 7 December 2006)
Corresponding author G. D. Housley: Department of Physiology, University of Auckland, Private Bag 92019, Auckland, New Zealand. Email: g.housley@auckland.ac.nz

Calcium homeostasis is central to the maintenance of sound transduction and auditory neurotransmission. Ca^{2+} has a range of effects on cochlear sensory hair cells, e.g. regulation of membrane conductances (Housley & Ashmore, 1992; Mammano & Ashmore, 1996; Raybould & Housley, 1997; Sridhar *et al.* 1997; Raybould *et al.* 2001; Housley *et al.* 2006), the transducer current (Mammano *et al.* 1999; Kennedy *et al.* 2003, 2005; Chan & Hudspeth, 2005), synaptic signalling (Evans *et al.* 2000; Beutner *et al.* 2001; Lioudyno *et al.* 2004), and outer hair cell (OHC) electromotility (Dallos *et al.* 1997; Frolenkov *et al.* 2000). The influx of Ca^{2+}, release of stored Ca^{2+}, and Ca^{2+} extrusion mechanisms (principally the plasma membrane calcium ATPases (PMCA)), act in concert to determine the spatiotemporal characteristics of Ca^{2+} signalling, which regulate cochlear hair cell function.

Transient receptor potential (TRP) ion channels represent a superfamily of non-selective cation channels which contribute to a wide range of cell functions, and have a particular significance in sensory systems (Clapham, 2003). The six mammalian subfamilies have been shown to exhibit polymodal activation (Ramsey *et al.* 2006). Expression of several members of the TRP channel family have been identified in cochlear tissues, including TRPA1 and TRPV4 (Corey, 2006). Canonical transient receptor potential (TRPC) channels are considered to be Ca^{2+} entry channels because of their high Ca^{2+} permeability, their association with store-coupled capacitative Ca^{2+} entry following discharge of intracellular Ca^{2+} stores, and store-independent Ca^{2+} entry (Clapham, 2003; Putney, 2004; Ramsey *et al.* 2006). TRPC channels are primary candidates for a Ca^{2+} entry pathway which can balance Ca^{2+} extrusion and establish Ca^{2+} homeostasis. A decrease in cytosolic Ca^{2+} ($[Ca^{2+}]_i$) activates TRPC channels (Mizuno *et al.* 1999). In recombinant expression models, the calmodulin-inositol trisphosphate receptor (IP_3R) binding domain (CIBD) has been shown to enable the binding of calmodulin

 DOI: 10.1113/jphysiol.2006.122929

to TRPC subunits and oppose channel activation (Tang *et al.* 2001; Zhang *et al.* 2001). Lowering $[Ca^{2+}]_i$ decreases calmodulin binding and thereby promotes Ca^{2+} entry. The restoration of $[Ca^{2+}]_i$ reverses this process. The seven TRPC subunits form tetrameric ion channels via homo- or heteromeric assembly. TRPC3, TRPC6, TRPC7 form a subfamily that can also be directly activated by the G protein-coupled receptor (GPCR) second messenger diacylglycerol (DAG) (Hofmann *et al.* 1999; Okada *et al.* 1999). TRPC3 channels are distinguishable by their regulation via tyrosine kinase-dependent phosphorylation (Vazquez *et al.* 2004; Kawasaki *et al.* 2006).

Here we have identified TRPC3 transcript and protein expression in cochlear hair cells, and characterized a novel TRPC-like Ca^{2+} entry pathway in cochlear OHCs. The Ca^{2+} entry current was activated by the lowering of cytosolic Ca^{2+} levels and had biophysical and pharmacological properties consistent with TRPC channels incorporating TRPC3 subunits. These data show that TRPC channel-mediated Ca^{2+} entry contributes to the restoration of OHC Ca^{2+} levels when $[Ca^{2+}]_i$ falls. The TRPC-mediated Ca^{2+} entry channels may also be directly activated by DAG to complement G protein-coupled receptor-mediated release of stored Ca^{2+}.

Method

All procedures were approved by the University of Auckland Animal Ethics Committee. The experiments used cochlear tissue obtained from rats and guinea pigs killed by an intraperitoneal injection of sodium pentobarbital (90 mg kg^{-1}, Nembutal, Abbott Laboratories).

RT-PCR detection of TRPC3 mRNA

TRPC3 mRNA expression was assessed using RT-PCR analysis of microdissected guinea pig and rat organ of Corti (two cochleae each), as previously described (Housley *et al.* 1999). Organ of Corti cDNAs were identified as positive for TRPC3 and prestin (an OHC specific gene marker; Zheng *et al.* 2000) by seminested PCR using the primer sets listed below. TRPC3 (Mizuno *et al.* 1999) sense (outer), GATGTGGTCTGAGTGCAAGGAGCTGTT; sense (inner), CCTGAGCGAAGTCACACTCCCAC; antisense, CCACTCTACATCACTGTCATCC; produced first and second round amplicons of 701 bp and 529 bp, respectively. Prestin sense (outer), ACGTGTGTTCCC-TAGGCGTCGGCCTCA; sense (inner), ACACTTCCT-CTGGGACTACTCCCACCC; antisense, GCCAGATGG-TCAACTCGATTTTGCTGGT; produced first and second round amplicons of 645 bp and 460 bp, respectively. In addition, single rat OHCs were aspirated using patch pipettes and expelled into 0.5 ml microfuge tubes in an 11 μl reaction mix. First strand cDNA synthesis was initiated by the addition of 0.5 μl of reverse transcriptase (Superscript II; Invitrogen, San Diego, CA, USA). The reaction proceeded for 1 h at 37°C after preincubations at 65°C, and then at 25°C for 10 min to promote random priming. A 3 μl cDNA mixture was used for seminested PCR amplification of TRPC3 and prestin. The 25 μl reaction mixtures for the first and second round amplifications were as described above. An aliquot (3 μl) was then re-amplified for an additional 50 cycles using the inner primer sets. PCR products (15 μl) were resolved on ethidium bromide-stained 2% agarose gels.

Immunofluorescence localization of TRPC3 protein

Confocal immunofluorescence microscopy was used to localize TRPC3 protein in whole-mount rat and guinea pig organ of Corti as previously described (Housley *et al.* 1999). Briefly, after fixation with 4% paraformaldehyde (BDH, England) in phosphate buffer (0.1 M, pH 7.4), the tissue was permeabilized using 0.5% Triton X-100 (BDH) in 0.1 M phosphate-buffered saline (PBS) for 30 min at room temperature and blocked overnight in PBS containing 2% bovine serum albumin (BSA; Sigma, Australia) and 5% normal goat serum (NGS; Vector Laboratories, Burlington, CA, USA). The immunolabelling utilized a polyclonal rabbit antimouse TRPC3 antibody (Alomone Laboratories, Israel) raised against a peptide corresponding to residues 822–835 in the TRPC3 intracellular C-terminus (accession no. Q9QZC1; Mori *et al.* 1998)). Western blot analysis recognized TRPC3 in rat brain (Alomone Laboratories). Control experiments included omission of the primary antiserum or preadsorption of the primary antiserum with the target antigen (7.5 μg ml^{-1}) at 4°C for 1 h. The anti-TRPC3 antiserum was used at a dilution of 1 : 100 or 1 : 250 in PBS containing 0.1% Triton X-100, 2% BSA and 5% NGS, and incubated at 4°C overnight. After washes in PBS, a Texas Red sulphonyl chloride-labelled secondary antibody (1 : 250 in PBS with 2% BSA, 5% NGS and 0.1% Triton X-100; affinity purified donkey antirabbit IgG; Jackson ImmunoResearch, PA, USA) was applied for 4–6 h at 4°C. Tissues were mounted (Citifluor; Agar Scientific, UK) after final washes, and imaged using a TCS SP2 laser scanning confocal microscope (Leica Microsystems, Germany) at 543 nm excitation, a 580 nm dichroic mirror and 600–700 nm band-pass filter.

Hair cell isolation and electrophysiology

OHCs were isolated from either the adult guinea pig or rat cochlea as previously described (Raybould & Housley, 1997). The organ of Corti was microdissected from either all, or selected turns of cochleae placed in a perilymph-like (standard) solution (composition (mM): NaCl, 150; KCl, 4.0; Na_2HPO_4, 8.0; NaH_2PO_4, 2.0; $MgCl_2$, 1.0; $CaCl_2$, 1.5; D-glucose, 4.0; osmolarity = 320 mosmol l^{-1}; pH 7.25

with NaOH). Following incubation in 0.5 mg ml^{-1} Trypsin (Gibco) for 10 min, the cells were triturated and placed in a 100 μl bath mounted on the stage of an inverted microscope (Nikon TMD, Japan) equipped with Nomarski DIC optics. Bath solutions were rapidly exchanged by a peristaltic pump (up to 850 $\mu l\ min^{-1}$; Gilson, France). All experiments were performed at room temperature (20–25°C).

Recording pipettes were made from borosilicate glass (GC120TF-10; Harvard Apparatus, UK) with a resistance of 2–5 MΩ (Model PB-7; Narishige, Japan) and filled with internal solution (composition (mM): KCl, 150; $MgCl_2$, 2.0; NaH_2PO_4, 1.0; Na_2HPO_4, 8.0; D-glucose, 3.0; $CaCl_2$ 0.01; EGTA, 0.5; osmolarity = 300 mosmol l^{-1}; pH 7.25). Whole-cell patch-clamp recordings were made using an Axopatch 200 patch-clamp amplifier (Molecular Devices, Sunnyvale, CA, USA) controlled by software (pCLAMP 8.0; Digidata 1200B Interface, Molecular Devices). Data were corrected for junction potential errors, which were 1.8 mV or less, except for the $Tris^+$ substitution experiments (−5.4 mV). Series resistance-derived voltage errors were reduced by adjustment of the voltage-clamp series resistance compensation to provide residual errors of <2 mV.

The current–voltage (I–V) relationship was obtained from voltage ramps (−100 to +50 mV, 1 s, holding potential (V_h) = −60 mV) repeated every 3 or 5 s as previously described (Raybould & Housley, 1997). The nominal Ca^{2+}-free external solution had a calculated residual 3.4 μM Ca^{2+}.

Sources of chemicals were: 2 aminoethyl diphenylborate (2APB), apamin, cyclopiazonic acid, 1-oleoyl-2-acetyl-*sn*-glycerol (OAG), dimethyl sulfoxide (DMSO), ruthenium red, Sigma; charybdotoxin, Alomone Laboratories; Tris-HCl, BDH; erbstatin analogue, Merck Biosciences.

Differences were considered statistically significant at $P < 0.05$ for paired and unpaired Student's t tests. Data are presented as the mean ± S.E.M.

Guinea pig OHC length ranged from 21.6 μm to 69.1 μm; average = 45.9 ± 1.2 μm (n = 245); average capacitance (C_M) = 18.2 ± 0.5 pF; average zero current potential (V_z) = −66.7 ± 0.8 mV. Rat OHC length ranged from 20.3 μm to 38.1 μm; average = 28.6 ± 0.9 μm (n = 45); average (C_M) = 12.1 ± 0.6 pF; average V_z = −63.9 ± 1.6 mV.

Confocal Ca^{2+} imaging

OHC intracellular Ca^{2+} levels were imaged using a Zeiss LSM410 inverted confocal microscope (Zeiss, Jenna, Germany), as previously described (Soeller & Cannell, 1996). Isolated OHCs were loaded with the Ca^{2+} indicator Fluo-3 (100 μM; Molecular Probes, OR, USA) included in the internal solution with EGTA omitted. Alternatively, dissected organ of Corti was incubated with Fluo-4 AM (5 μM; Molecular Probes) in standard extracellular solution, for 30 min prior to cell trituration. DMSO (1.8%) was used to aid the solubility of OAG. DMSO at this concentration had no effect on OHC membrane conductance. The fluorescent indicators were excited by an argon ion laser at 488 nm (Uniphase, San Jose, CA, USA), and emitted light was collected by a 40× water immersion objective (NA 1.2, Zeiss) and detected at 535 ± 25 nm. Data are displayed as fluorescence at a given time/resting fluorescence immediately prior to the evoked changes in $[Ca^{2+}]_i$. Data processing was performed using custom routines (Interactive Data Language, Research Systems Inc., Boulder, CO, USA).

Results

Detection of TRPC3 mRNA expression in the organ of Corti

TRPC3 mRNA was detected in guinea pig and rat organ of Corti by RT-PCR (Fig. 1*A* and *B*). The organ of Corti cDNAs were also positive for prestin, the OHC

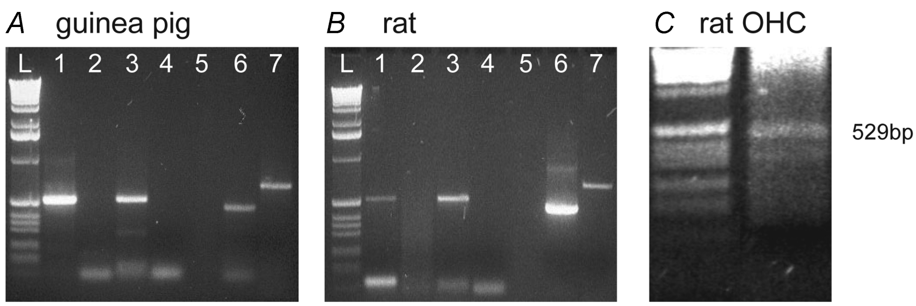

Figure 1. RT-PCR detection of TRPC3 mRNA
A and *B*, PCR amplicons from guinea pig and rat tissues. In each panel, lanes show: L, ladder; 1, organ of Corti TRPC3 + RT; 2, TRPC3 – RT; 3, cerebellum TRPC3 + RT; 4, no template control; 5, blank; 6, organ of Corti prestin + RT; 7, organ of Corti β-actin + RT. Semi-nested PCR; *TRPC3* cDNA = 529 bp; prestin cDNA = 460 bp; β-actin cDNA = 660 bp. *C*, single-cell RT-PCR confirming TRPC3 expression by rat outer hair cells (left lane = ladder).

electromotility protein (Zheng *et al.* 2000), and for β-actin (López-Candales *et al.* 1995). The identity of the 529 bp TRPC3 amplicon in guinea pig organ of Corti was confirmed by direct sequencing. The guinea pig TRPC3 cDNA amplicon (accession no. AB090949) included substitutions: C1464G; G1465A; A1467G; C1477A, compared with the rat homologue (accession no. NM021771; Mizuno *et al.* 1999). Expression of the TRPC3 transcript in individual rat OHCs was confirmed by single cell RT-PCR (Fig. 1*C*), using prestin as a positive control. Three rat OHCs were confirmed as positive for TRPC3. Negative controls with no template, or omission of reverse transcriptase, showed no amplicon.

TRPC3 immunolocalization to cochlear hair cells

TRPC3 immunofluorescence labelling was localized to the OHCs and IHCs where it had a pronounced bipolar distribution (Fig. 2, 13 rat and 3 guinea pig experiments). Labelling was absent in the supporting cells and pillar cells. In OHCs, TRPC3 antibody labelling was predominantly in both the cell wall and cytoplasm immediately below the cuticular plate, and at the plasma membrane of the synaptic region beneath the nucleus (Fig. 2*A*–*C*). No labelling of the stereocilia was detected, however, discrete labelling occurred within the cuticular plate (Fig. 2*C*) at the site of regression of the kinocilium. IHC TRPC3 labelling was comparable to that of OHCs. Omission of the primary antibody or preadsorption with the target epitope peptide blocked the immunolabelling (Fig. 2*A* and *B* insets).

Outer hair cell currents enabled by lowering [Ca^{2+}]

Given the ability of TRPC channels to mediate Ca^{2+} entry following reductions in [Ca^{2+}]$_i$ (Mizuno *et al.* 1999), guinea pig and rat OHCs were exposed to a Ca^{2+} conditioning protocol known to deplete [Ca^{2+}]$_i$ (Ashmore & Ohmori, 1990) (see also Fig. 8*A*–*C*). OHCs were initially superfused with an extracellular solution containing 1.5 mM Ca^{2+} (Ca$_o^{2+}$) (see Methods) until membrane currents were steady (Fig. 3*A* and *B*). Exposure to a nominally Ca^{2+}-free solution reduced voltage-dependent membrane current as previously described (Raybould & Housley, 1997). The subsequent return of the Ca^{2+}-containing solution elicited a transient overshoot in the outward current, accompanied by a progressive increase in inward current (arrows, Fig. 3*A* and *B*). The inward current component, activated over tens of seconds, was seen in 165 out of 187 guinea pig OHCs and in 28 out of 45 rat OHCs. This current subsequently declined over several minutes (not shown). The current response was robust and could be generated several times in individual guinea pig and rat OHCs by the repeated cycling of [Ca^{2+}]. The current response was unaffected when the Mg^{2+} concentration was maintained at 2.5 mM throughout the experiment ($n = 4$). Initial experiments included continuous video recording of the

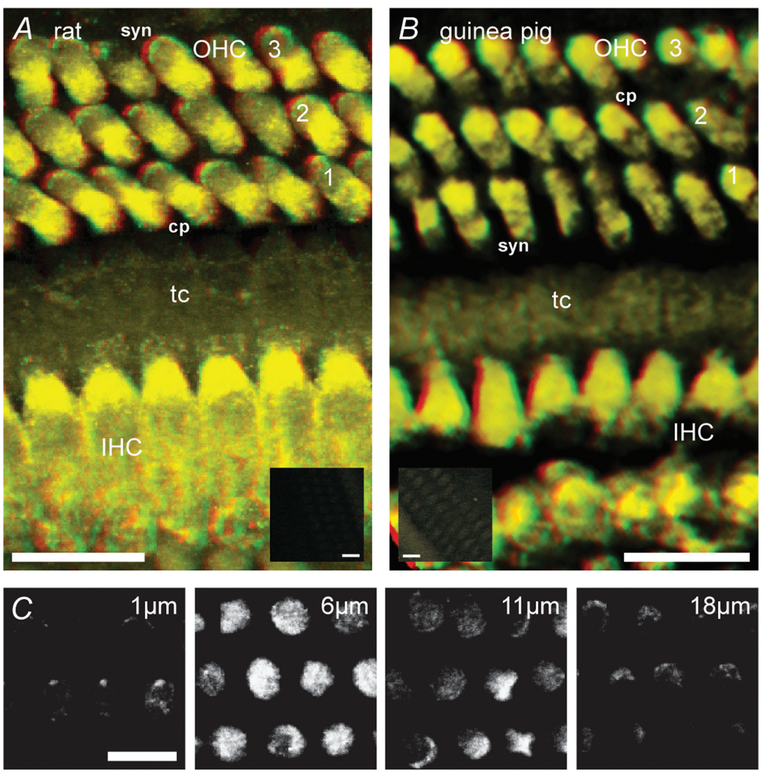

Figure 2. TRPC3 confocal immunofluorescence in outer (OHC) and inner hair cells (IHC) from rat and guinea pig organ of Corti
A and *B*, anaglyph (red (left eye)/green (right eye)) stereoimages constructed from stacks of optical sections taken though whole-mount organ of Corti. Note labelling in the cuticular plate (cp) – upper third of the cell and also in the basal (synaptic, syn) region of both sensory cell types. tC, tunnel of Corti – showing absence of labelling of pillar cells. Insets are comparable stereoimages obtained using image stacks from control tissue; Inset *A* is a peptide block of rat organ of Corti immunolabelling; Inset *B* is a control for guinea pig organ of Corti where the primary antibody was omitted. Scale bars = 10 μm, except for insets (30 μm). *C*, detail of rat OHC labelling from a series of optical sections; the depth of each section from the apical surface is indicated. The greatest density of labelling occurred within approximately 6 μm of the cuticular plate and also in the basal synaptic region.

OHC. *Post hoc* analysis of these data (after Housley *et al.* 1995) showed that there was no significant change in OHC volume during the cycling of Ca_o^{2+} (OHC volume in standard solution = 4.1 ± 0.7 pl; volume in Ca^{2+}-free solution = 3.8 ± 0.7 pl; volume at peak of inward current = 3.8 ± 0.6 pl; $P > 0.05$; Student's paired *t* tests; $n = 4$). These data are consistent with the activation of a TRPC-like current (subsequently referred to as the TRPC current). The data described below provide evidence that discriminates this TRPC current from other members of the TRP channel superfamily, including TRPA1 and TRPV4 which are known to be expressed in OHCs (Liedtke *et al.* 2000; Corey *et al.* 2004; Kwan *et al.* 2006; Shen *et al.* 2006).

The Ca^{2+} dependency of the TRPC current response was analysed by varying the restoration $[Ca^{2+}]_o$ subsequent to the lowering of $[Ca^{2+}]_i$ using the Ca^{2+}-free solution as described. These experiments showed that the underlying inward current component of the response, measured at −90 mV, was dependent upon the presence of Ca_o^{2+}, and that the amplitude of the current progressively increased with higher $[Ca^{2+}]_o$ (Fig. 4*A*). In contrast, the outward current component had a sigmoidal $[Ca^{2+}]_o$ dependency with an $EC_{50} = 462$ μM (Fig. 4*B*). This is consistent with Ca_o^{2+} regulating the gating of the underlying TRPC inward current and the rapid secondary activation of $I_{K,Ca}$, which saturates at physiological $[Ca^{2+}]_o$ levels.

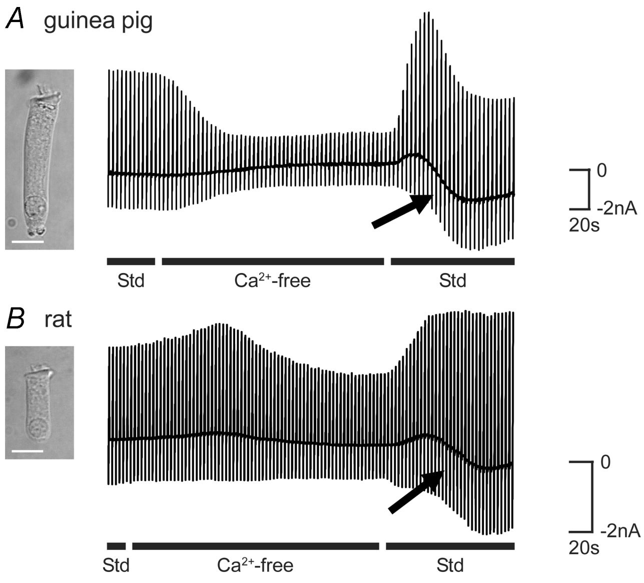

Figure 3. TRPC currents in guinea pig and rat OHCs
A, chart record of guinea pig OHC membrane current in response to repeated voltage ramps (−100 to + 50 mV, 1 s, every 3 s, $V_h = -60$ mV) during the sequential superfusion of standard (Std; including 1.5 mM Ca_o^{2+}), nominally Ca^{2+}-free, and return of Std solutions. Removal of Ca_o^{2+} produced a reduction in membrane current. The subsequent restoration of Ca_o^{2+} produced a biphasic current response. The baseline current record (at V_h) shows the time course for activation of an underlying TRPC inward current with restoration of Ca^{2+} (see arrows). *B*, chart record of rat OHC membrane current during the cycling of Ca_o^{2+} shows a similar recruitment of currents with the restoration of Ca_o^{2+}. Scale bars = 10 μm.

Pharmacological separation of Ca^{2+}-dependent currents

The outward current component, activated by the restoration of Ca_o^{2+}, was inhibited by the K_{Ca} channel blockers apamin and charybdotoxin, revealing the TRPC inward current component (Fig. 5). The small-conductance K_{Ca} channel (SK) blocker apamin (1 μM; Yamamoto *et al.* 1997) produced a moderate reduction in the Ca^{2+} depletion-induced overshoot

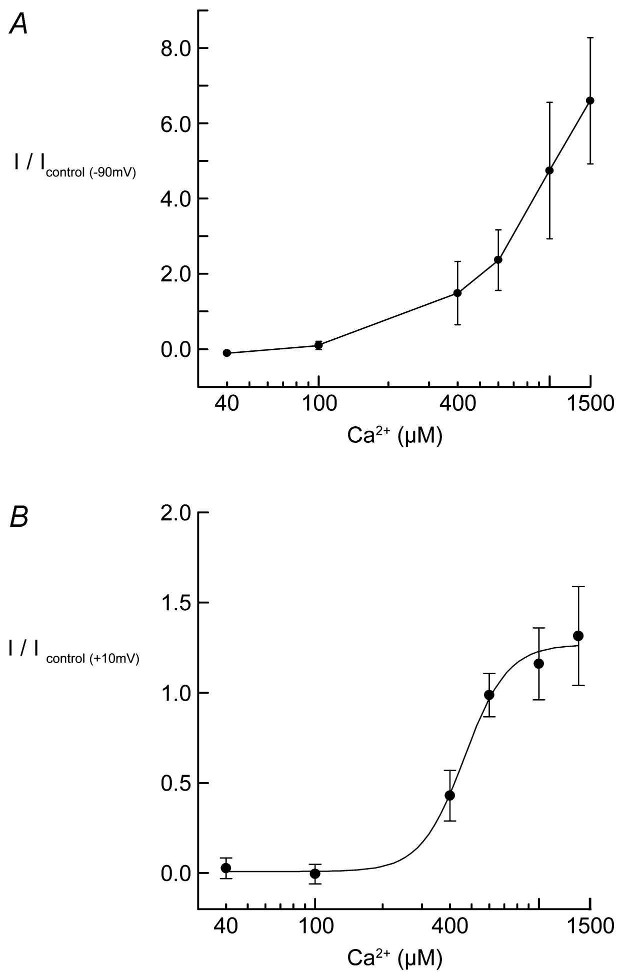

Figure 4. Dependency of TRPC current activation on $[Ca^{2+}]_o$ in guinea pig OHCs
A, $[Ca^{2+}]_o$ dependency of the TRPC inward current during the cycling of Ca_o^{2+}. Peak inward current was measured at −90 mV (close to E_K) following the return of varying concentrations of Ca_o^{2+}. *B*, dependency of secondary $I_{K,Ca}$ on $[Ca^{2+}]_o$ was assessed by measuring the peak outward current at +10 mV during cycling with varying $[Ca^{2+}]_o$. Data fitted by a Boltzman equation with $EC_{50} = 462$ μM and maximum recruitment of $I_{K,Ca}$ at ∼1.5 mM Ca_o^{2+}. Each data point represents a mean ± S.E.M. for independent experiments (n = 3–8).

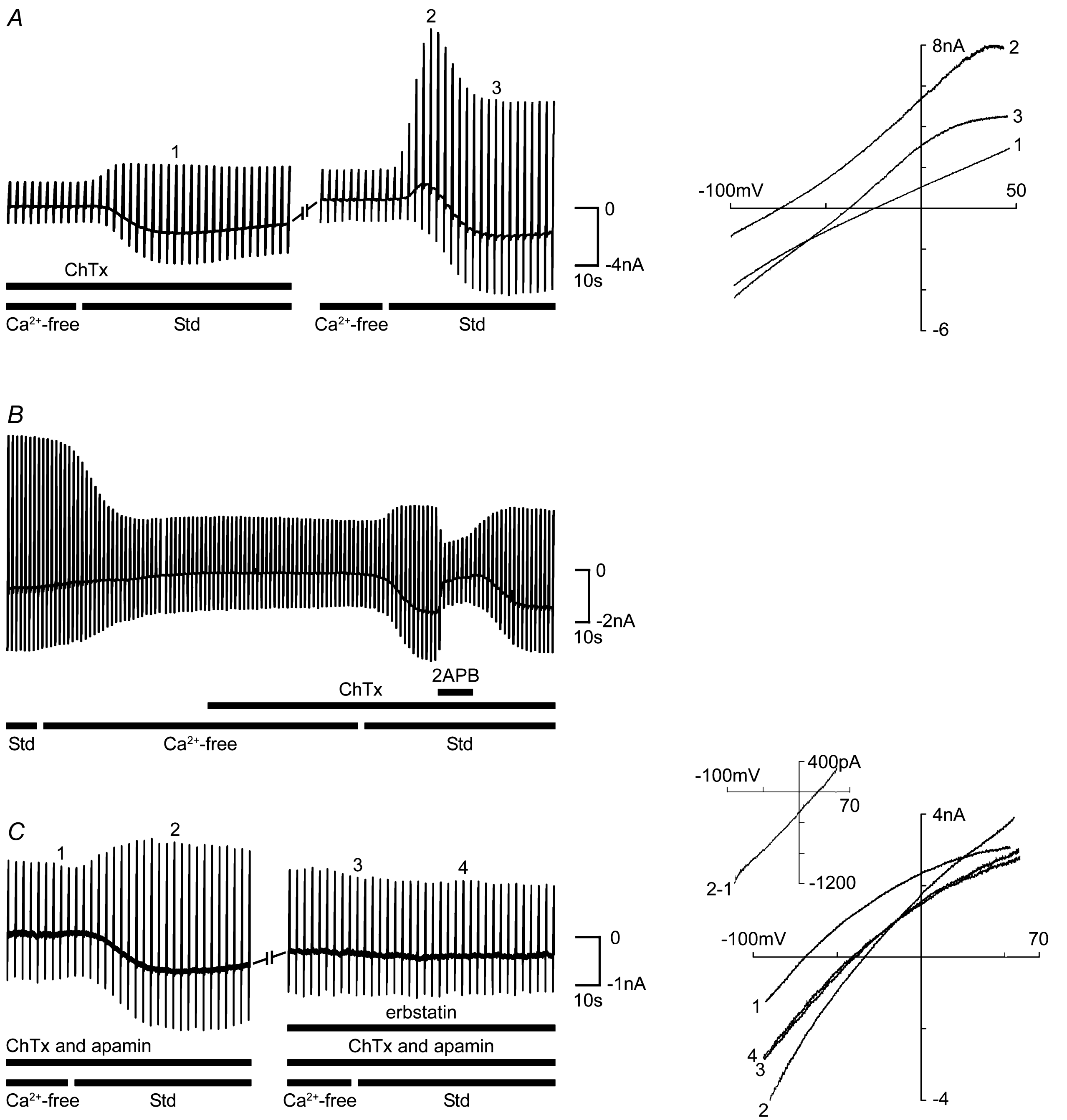

Figure 5. Pharmacology of TRPC currents

A, left panel shows chart record of guinea pig OHC membrane currents during repeated voltage ramps (–100 to +50 mV, 1 s, every 3 s, $V_h = -60$ mV) during the cycling of Ca^{2+}_o. ChTx (100 nM) largely blocked the recruitment of outward current (76%) with the restoration of Ca^{2+}_o (Std; including 1.5 mM Ca^{2+}_o) and revealed the development of the underlying TRPC inward current. This block was reversible with washout. Right panel shows examples of *I–V* relationships that were derived by plotting the marked current traces elicited by the voltage ramps: (1) peak of the TRPC inward current; (2) peak of the secondary $I_{K,Ca}$ (TRPC3 current masked by recruited K^+ current); (3) peak TRPC inward current with $I_{K,Ca}$. *B*, in the presence of ChTx, the TRPC current was reversibly blocked by the local application of 2-aminoethyl diphenylborate (2APB; 1 mM). *C*, in the presence of apamin (1 μM) and charybdotoxin (400 nM), erbstatin analogue (100 μM) blocked the TRPC inward current, which was evident in the preceding cycling of Ca^{2+}_o. Right panel (inset) shows the *I–V* of the isolated TRPC current (2 – 1), obtained by subtracting the control *I–V* (1) from the *I–V* at the peak of the inward current response (2); 3, 4, nominally Ca^{2+}-free control and with the restoration of Ca^{2+}_o (Std) *I–V* relationships in the presence of erbstatin analogue. Note that the TRPC current $E_{rev} = +32$ mV (*I–V* inset, trace 2 – 1).

in guinea pig OHC membrane current (mean = 24%, $n = 7$, data not shown). Following washout of apamin, the larg-conductance K_{Ca} channel (BK) blocker charybdotoxin (ChTx, 100 nM to 1 μM; Nenov *et al.* 1997) blocked the majority of the outward current component (mean = 76%, $P < 0.05$; $n = 4$). The ChTx-mediated block was reversible with washout (Fig. 5*A*). In rat OHCs, the outward current response was reduced by 28% by apamin ($n = 9$), and 85% by ChTx ($n = 2$).

It has been reported that TRPC channels are blocked by 2APB (Lievremont *et al.* 2005). As shown in Fig. 5*B*, application of 2APB (1 mM) in the presence of ChTx (1 μM; $n = 3$) produced a marked decrease in the TRPC current components that was reversible upon washout. Inclusion of 2APB in the internal solution (1 mM) did not block the TRPC current response (data not shown).

Erbstatin analogue, a tyrosine kinase inhibitor which selectively antagonizes TRPC3 channel activation (Vazquez *et al.* 2004) was used to further consolidate the characterization of the TRPC current. Figure 5*C* shows that erbstatin analogue (100 μM) blocked the OHC current response induced by the cycling of Ca^{2+} in the presence of ChTx and apamin (both 1 μM). This block was irreversible for up to 1.5 hours and eight iterations of Ca^{2+} cycling. Erbstatin analogue blocked the TRPC inward currents by 91.7 ± 4.3% (100 μM, $n = 6$; $V_h = -60$ mV). Erbstatin analogue had no effect on the control OHC currents in the Ca^{2+}-free solution. In the absence of K_{Ca} channel blockers, erbstatin analogue produced a block of both the inward current (84.5 ± 6.7% at 100 μM, $n = 4$; 93.8 ± 3.0% at 400 μM, $n = 2$; $V_h = -60$ mV) and secondary K_{Ca} outward current elicited by the restoration of Ca_o^{2+} (data not shown).

The TRPC currents were studied in a range of OHCs isolated from all turns of the guinea pig cochlea. In the presence of the K_{Ca} channel blockers apamin (1 μM) and ChTx (400 nM), the restoration of Ca_o^{2+} elicited a mean inward current of −721 ± 74 pA ($n = 36$; $V_h = -60$ mV) (see trace 2 in Fig. 5*C*). This produced an average depolarizing shift in zero-current potential (V_z) of +22.5 ± 1.8 mV measured from the current–voltage (*I–V*) relationship (compare Fig. 5*A*, *I–V* traces 1 and 2). The *I–V* relationship of the TRPC current elicited by the restoration Ca_o^{2+} (Fig. 5*C*, *I–V* inset) was derived by subtracting the *I–V* in the Ca^{2+}-free solution with ChTx and apamin (Fig. 5*C*, *I–V* trace 1) from the *I–V* at the peak of the inward current (Fig. 5*C*, *I–V* trace 2). The TRPC current had a linear *I–V* relationship, with a mean reversal potential ($TRPC3_{E_{rev}}$) of +21.7 ± 3.0 mV (Fig. 5*C* *I–V* inset; $n = 35$).

The TRPC inward current was correlated with the tonotopically related background conductance (Fig. 6). The TRPC currents were largest in the shorter OHCs, which have higher background membrane conductances. It has previously been shown that OHC membrane conductance increases progressively from the apical (low-frequency) turn towards the basal (hig-frequency) turns of the guinea pig cochlea (Housley & Ashmore, 1992; Mammano & Ashmore, 1996; Raybould & Housley, 1997). The average specific TRPC current (I_{TRPC} at V_h normalized to C_m) increased ∼3-fold with increasing specific membrane conductance (measured about −75 mV).

Given the composition of intracellular and extracellular solutions, the positive $TRPC3_{E_{rev}}$ of ∼+ 22 mV is consistent with a channel more selective for Na^+ than K^+. The relative permeability of the TRPC channel was determined by replacing Na_o^+ with $Tris^+$. Local application of a solution including 36 mM Na^+ and 140 mM $Tris^+$ immediately reduced the TRPC inward current and produced a mean hyperpolarizing shift in V_z of −13.5 ± 3.8 mV ($n = 4$) (Fig. 7). The *I–V* relationship of the isolated TRPC current, obtained by subtracting the fully corrected *I–V* from the preceding control *I–V*, showed a shift in E_{rev} of −7.0 ± 3.2 mV (Fig. 7 *I–V* inset). From the Goldman–Hodgkin–Katz equation, this suggests a non-selective cation permeability ratio of $P_{Na} : P_K$ 1 : 0.6, and is consistent with the results of Na^+ substitution experiments with recombinant TRPC3 channels (Lintschinger *et al.* 2000). While TRPC3 channels conduct a Ca^{2+} current, the recording of this is problematic, even in recombinant expression systems. However, Ca^{2+} imaging confirmed that TRPC-mediated Ca^{2+} entry in OHCs was primed by lowering $[Ca^{2+}]_i$.

Imaging of TRPC channel-mediated Ca^{2+} influx

Simultaneous Ca^{2+} imaging and whole-cell patch-clamp recordings from guinea pig OHCs confirmed rapid Ca^{2+}

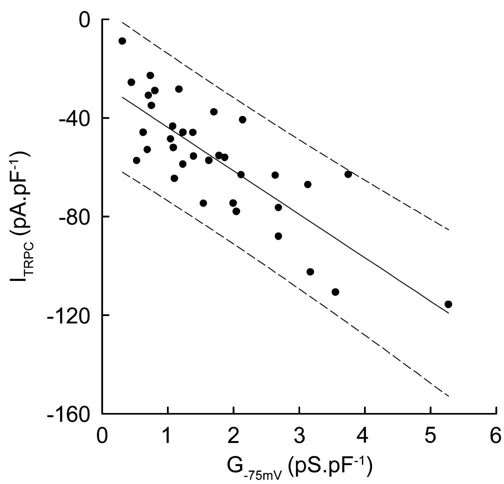

Figure 6. Tonotopic variation in TRPC inward current
Normalized guinea pig OHC TRPC inward current ($V_h = -60$ mV, normalized to C_m) elicited by the cycling of Ca_o^{2+}, was positively correlated with OHC-specific membrane conductance ($G_{-75\ mV}$, normalized to C_m). Data are fitted by linear regression with 95% confidence intervals, $R = 0.8$.

entry followed the restoration of Ca^{2+}_o. Intracellular dialysis with the Ca^{2+} indicator Fluo-3 (100 μM) took approximately 5 min to reach a steady level of fluorescence in the Ca^{2+}-containing solution. Superfusion of the nominally Ca^{2+}-free solution produced a decrease in the $[Ca^{2+}]_i$ fluorescence signal over approximately 2 min, with a concomitant reduction in $I_{K,Ca}$ (Fig. 8*A*; $n = 5$). The subsequent restoration of Ca^{2+}_o elicited both a rapid overshoot in $[Ca^{2+}]_i$ and a coincident recruitment of $I_{K,Ca}$ (Fig. 8*A*).

Superfusion with the sarcoplasmic/endoplasmic reticulum calcium ATPase (SERCA) pump blocker cyclopiazonic acid (CPA; 10 μM; $n = 7$) in standard solution, caused an increase in membrane (K_{Ca}) conductance consistent with the release of stored Ca^{2+}. However, the presence of CPA during the cycling of Ca^{2+}_o had no obvious effect on the TRPC current response (data not shown), suggesting that in OHCs the TRPC current is not coupled to intracellular Ca^{2+} stores. Similarly, ruthenium red (100 μM), an antagonist of Ca^{2+} store signalling (Zucchi & Ronca-Testoni, 1997) and TRPV4 receptors (Shen *et al.* 2006), failed to block the OHC TRPC current response when included in the recording electrode ($n = 6$ rat OHCs, data not shown).

As predicted by the block of the TRPC inward current by the selective antagonist erbstatin analogue, confocal Ca^{2+} imaging with Fluo-4 AM showed that erbstatin analogue blocked the increase in $[Ca^{2+}]_i$ elicited by the restoration of Ca^{2+}_o (Fig. 8*B* and *C*). These experiments reconciled the electrophysiological characterization of a TRPC inward current with direct measurement of Ca^{2+} influx. Restoration of Ca^{2+}_o invoked an overshoot in $[Ca^{2+}]_i$ with a mean F/F_0 of 1.35 ± 0.07 ($n = 6$) (Fig. 8*C*). A second cycling of $[Ca^{2+}]$ resulted in a Ca^{2+} influx which did not significantly vary from the first response in control experiments, but whuch was reduced by 72% in the presence of erbstatin analogue (mean $F/F_0 = 0.33 \pm 0.07$; $P < 0.01$, Student's paired *t* test).

Second messenger activation of TRPC-mediated Ca^{2+} entry

Ca^{2+} entry channels assembled from TRPC3 subunits can be activated either by modulation of $[Ca^{2+}]_i$ or directly by DAG, a second messenger in the GPCR-PLC signalling pathway (Hofmann *et al.* 1999; Okada *et al.* 1999; Lintschinger *et al.* 2000; Ma *et al.* 2000). In guinea pig OHCs, bath application of 1-oleolyl-2-acetyl-*sn*-glycerol (OAG; an analogue of DAG; 100 μM to 1 mM; $n = 14$) in standard solution produced a dose-dependent increase in membrane current (Fig. 8*D*). In the absence of extracellular Ca^{2+}, OAG had no effect. In control

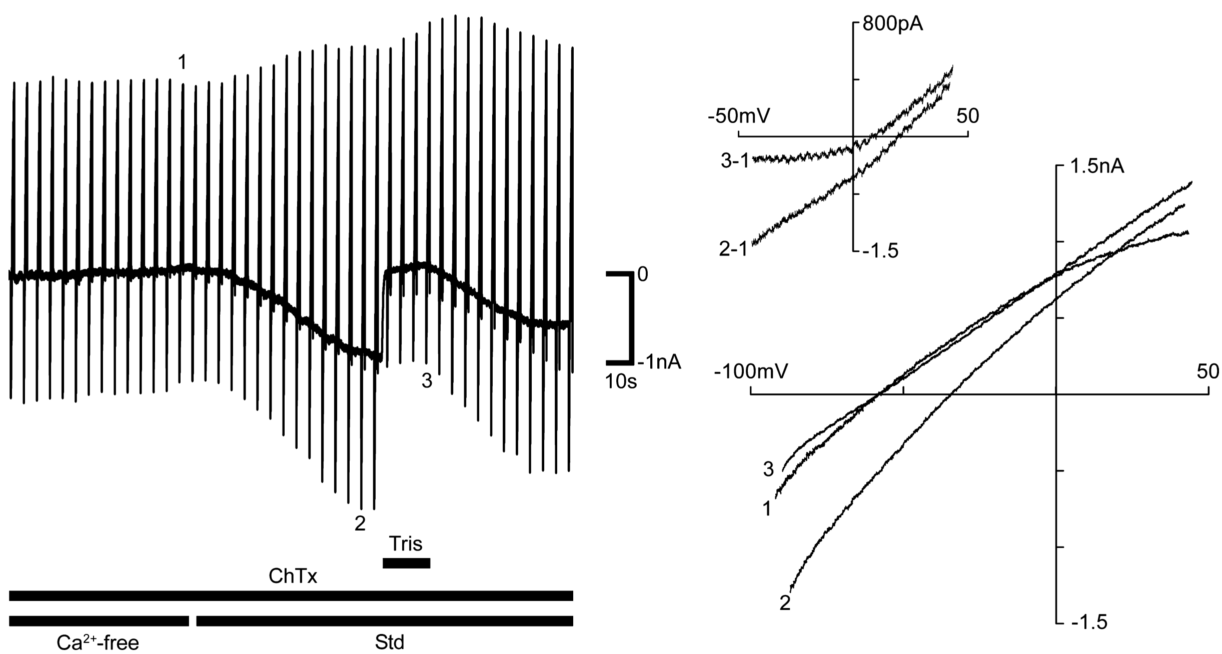

Figure 7. The TRPC inward current is largely borne by Na^+
The inward current elicited by the cycling of Ca^{2+}_o was blocked by focal application of a solution with $Tris^+$ (140 mM) replacing the majority of Na^+. Left panel shows chart record of guinea pig OHC current in response to repeated voltage ramps (–100 to +50 mV, 1 s, every 3 s, $V_h = -60$ mV). Right panel shows *I–V* relationships for representative traces just prior to restoration of Ca^{2+}_o (Std; including 1.5 mM Ca^{2+}_o) (1), at the peak of the TRPC inward current (2) and during the block of this current by $Tris^+$ (3). The inset shows the leftward shift in E_{rev} of the isolated TRPC currents calculated by subtracting the control *I–V* from the *I–V* after activation of the TRPC current.

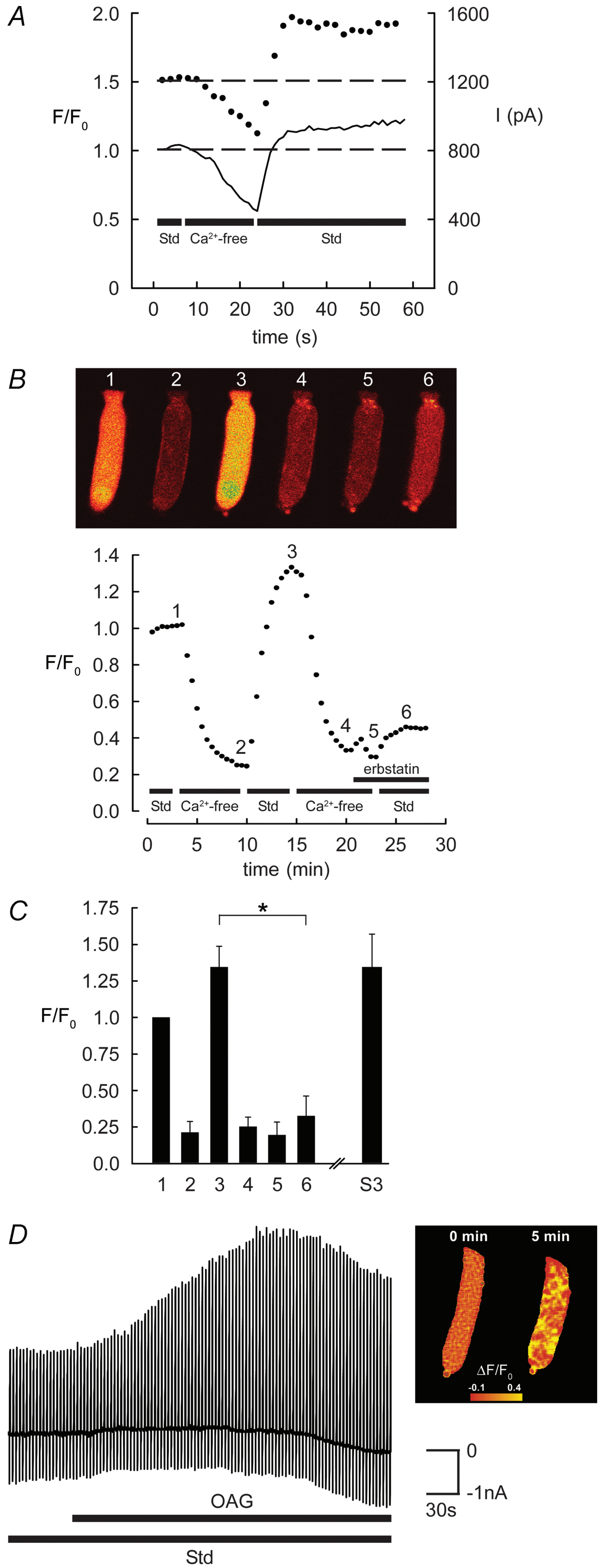

experiments, bath superfusion of the carrier DMSO alone produced no significant change in membrane current (data not shown). Confocal Ca^{2+} imaging confirmed that OAG increased $[Ca^{2+}]_i$ (1 mM OAG; $n = 3$; Fig. 8*D*). The OAG-mediated increases in both OHC membrane conductance and Ca_i^{2+} developed over several minutes.

Discussion

This study characterizes a TRPC Ca^{2+} entry current in guinea pig and rat outer hair cells which is activated by the lowering of Ca^{2+} levels following exposure to nominally Ca^{2+}-free solution, and may provide a homeostatic mechanism that returns $[Ca^{2+}]_i$ to a set-point over a period of minutes. The conductance activated over seconds once Ca^{2+} was returned to the bathing solution, and led to the restoration of intracellular Ca^{2+} levels. Outward K^+ current was rapidly recruited by the TRPC current, indicating a close coupling between the Ca^{2+} entry channels and K_{Ca} channels. The TRPC Ca^{2+} entry current was also activated by the DAG second messenger pathway, and is therefore positioned to augment G protein-coupled Ca^{2+} signalling in these cells. The pharmacological and biophysical characterization of the OHC Ca^{2+} entry current matches the phenotype of TRPC ion channels that incorporate TRPC3 subunits. The assignment of the OHC Ca^{2+} entry current to TRPC3-like channels was supported by RT-PCR and confocal immunofluorescence experiments, which identified strong TRPC3 expression in the hair cells, with a bipolar distribution of the TRPC3

Figure 8. TRPC channel-mediated Ca^{2+} entry in guinea pig OHCs
A, simultaneous Ca^{2+} imaging (Fluo-3) and whole-cell patch-clamp recordings show that the removal of Ca_o^{2+} decreased $[Ca^{2+}]_i$ and reduced $I_{K,Ca}$. The subsequent return of Ca_o^{2+} (Std; including 1.5 mM Ca_o^{2+}) produced an overshoot in both $[Ca^{2+}]_i$ and $I_{K,Ca}$ (dashed line shows membrane current at +10 mV; continuous line Ca_i^{2+}). *B* and *C*, Ca^{2+} imaging (Fluo-4 AM) showing the block of the TRPC-mediated Ca^{2+} influx by erbstatin analogue (100 μM). From a reference level (1), superfusion of the nominally Ca^{2+}-free solution produced a large decrease in emitted fluorescence (2). The restoration of Ca_o^{2+} (3) resulted in an overshoot in $[Ca^{2+}]_i$ (combined data, $n = 6$). Subsequent cycling of Ca_o^{2+}, with erbstatin analogue inhibited the response ($n = 3$) (6), compared with the repeatable TRPC-mediated overshoot in $[Ca^{2+}]$ (S3; $n = 3$). Erbstatin analogue largely blocked the restoration of $[Ca^{2+}]_i$ (*$P < 0.05$ in *C*); compare images (3) and (6) in *B*. *D*, direct activation of TRPC channels by 1-oleolyl-2-acetyl-*sn*-glycerol (OAG) in guinea pig OHCs. Bath superfusion of OAG (1 mM) in standard (Std) solution recruited OHC $I_{K,Ca}$, consistent with Ca^{2+} influx through TRPC channels. Chart record of membrane currents elicited by repeated voltage ramps as previously described. The OAG-mediated increase in guinea pig OHC Ca^{2+} levels was confirmed by confocal fluorescence imaging using Fluo-4 AM (right panel). OHC fluorescence intensity was determined as the change in ratio relative to the fluorescence signal prior to the application of OAG.

protein at the apical transduction and basal synaptic poles.

The development of the slowly activating inward current in OHCs following depletion of cytosolic Ca^{2+} by exposure to low-Ca^{2+} solution is consistent with regulation of TRPC channel activation via calmodulin binding (Mizuno *et al.* 1999; Tang *et al.* 2001; Zhang *et al.* 2001). In addition, our observation that the OHC TRPC inward current, although largely borne by Na^+, requires Ca_o^{2+} (see Fig. 4*A*), is consistent with previous voltage-clamp studies of recombinant TRPC3 channels (Lintschinger *et al.* 2000). Similarly, the putative TRPC current in OHCs exhibited little rectification and a positive reversal potential indicative of a significant selectivity for Na^+, as seen with recombinant TRPC3 homomeric and TRPC3/TRPC1 heteromeric Ca^{2+} entry channels (Lintschinger *et al.* 2000; Strubing *et al.* 2001; Hofmann *et al.* 2002). The OHC TRPC current was rapidly blocked by extracellular 2APB, comparable to the block of recombinant TRPC3 channels (Ma *et al.* 2000; Trebak *et al.* 2002). The use of the tyrosine kinase inhibitor erbstatin analogue provided the strongest pharmacological evidence that the OHC Ca^{2+} entry pathway is attributable to TRPC3 channels (Vazquez *et al.* 2004). Erbstatin analogue blocked both the Ca^{2+} depletion-activated OHC inward current and re-entry of Ca^{2+}.

It seems likely, from our experiments, that TRPC-mediated Ca^{2+} entry establishes a 'set-point' for OHC $[Ca^{2+}]_i$ by balancing (via negative feedback control of TRPC channel activation) Ca^{2+} extrusion mechanisms such as the plasma membrane CaATPase (PMCA) (Dumont *et al.* 2001). Our data indicate that a fall in $[Ca^{2+}]_i$ below the reported resting levels of ~100 nM (Ashmore & Ohmori, 1990) would activate TRPC channel Ca^{2+} entry and restore $[Ca^{2+}]_i$. Dialysis of the cell with the modest Ca^{2+} buffering provided by 0.5 mM EGTA did not appear to activate TRPC current.

In OHCs, we used OAG to show that Ca^{2+} entry could be directly activated by the GPCR–Gq–PLC–PiP_2–DAG pathway, as reported for recombinant TRPC3 channels (Hofmann *et al.* 1999; Zitt *et al.* 2002). The production of DAG in the OHC plasma membrane is a previously unconsidered component of the P2YR–Gq–PLC_β pathway that promotes the release of Ca^{2+} from IP_3R-sensitive stores of Hensen's body found in the subcuticular plate region of guinea pig OHCs (Mammano *et al.* 1999; Okamura *et al.* 2001). Direct activation of TRPC-mediated Ca^{2+} entry by DAG may also contribute to OHC efferent regulation through the Gq-linked M_3 muscarinic receptor (Khan *et al.* 2002). However the dominant cholinergic efferent effect on OHCs is via the α_9/α_{10} nicotinic receptor, where Ca^{2+} entry and associated Ca^{2+}-induced Ca^{2+} release recruits the SK conductance within hundreds of milliseconds to hyperpolarize the cells (Housley & Ashmore, 1991; Evans *et al.* 2000; Oliver *et al.* 2000; Lioudyno *et al.* 2004). The TRPC channel Ca^{2+}-entry pathway may also contribute to regulation of afferent synaptic neurotransmission. In cochlear hair cells, Ca_i^{2+} affects the rate and magnitude of vesicle exocytosis and endocytosis (Beutner *et al.* 2001), and the interaction between ryanodine-sensitive Ca^{2+} stores and BK channels, which inhibits IHC synaptic transmission (Beurg *et al.* 2005). The immunolocalization of TRPC3 in the basal region of OHCs matches that of the BK and SK channels (Oliver *et al.* 2000; Hafidi *et al.* 2005) and implies a spatial coupling with these K_{Ca} channels. Our voltage-clamp experiments clearly demonstrate a close coupling between the OHC TRPC Ca^{2+} entry pathway and the apamin-sensitive SK channels and ChTx-sensitive BK channels. The BK channels in particular were shown to have a major influence on OHC membrane filter properties by our manipulation of Ca^{2+} extrusion and Ca^{2+} entry. Figure 5*A* shows that the BK conductance is recruited about 5 s after the restoration of Ca_o^{2+}. This delay is similar to the onset of the underlying (TRPC) inward current and is consistent with the low threshold for $[Ca^{2+}]_o$ required to activate BK through this mechanism. The BK conductance was fully activated within 20 s in the example shown, whereas maximal activation of the TRPC inward current took twice as long.

As noted, expression of other members of the TRP channel superfamily has been shown in hair cells (Corey, 2006). However, the pharmacological properties of these channels (Ramsey *et al.* 2006) are incompatible with those of the OHC TRPC current reported here. TRPV4 expression has been identified in the hair cells and stria vascularis (Liedtke *et al.* 2000; Shen *et al.* 2006) where TRPV4 currents were activated by hypoosmotic stress and the phorbol ester 4-α-phorbol 12,13-didecanoate (4α-PDD) (Shen *et al.* 2006). TRPV4 currents are known to be potentiated with rises in $[Ca^{2+}]_i$ (Strotmann *et al.* 2003). In contrast, the OHC TRPC current appeared to be independent of changes in cell volume, and reduces as $[Ca^{2+}]_i$ rises. TRPA1 channels have been localized to the tip regions of the stereocilia (Kwan *et al.* 2006) where coupling with K_{Ca} channels would not occur. 2APB provides an effective block of TRPC current, and is a standard tool for functional analysis of recombinant TRPC channels (Trebak *et al.* 2002; Lievremont *et al.* 2005). However, 2APB may also inhibit IP_3R-gated Ca^{2+} release (Maruyama *et al.* 1997) and can affect several types of ion channels differently (Hu *et al.* 2004; Lemonnier *et al.* 2004). We noted a small reduction in background conductance by 2ABP in addition to the block of the TRPC current. Erbstatin analogue is a better discriminator for TRPC3 channels, as it inhibits non-receptor tyrosine kinase phosphorylation of TRPC3 channels, which is integral to their activation (Vazquez *et al.* 2004), but not other TRPC channels (Kawasaki *et al.* 2006). While erbstatin analogue may block KCNQ-type channels (Gamper *et al.* 2003), under our experimental conditions erbstatin analogue had no effect on the background conductance (see Fig. 5*C*), which would be largely mediated by KCNQ4 channels (Marcotti & Kros, 1999). Furthermore, we have directly demonstrated that erbstatin analogue blocks Ca^{2+} entry. Thus, while we cannot exclude the contribution of additional TRPC subunits to the TRPC channel, our data strongly implicate a functional role for the TRPC3 subunit. Full resolution of the molecular physiology of TRPC channels in OHCs will require screening for additional TRPC transcripts and proteins, advances in TRPC channel pharmacology, and subunit-specific manipulation of TRPC gene expression in animal models.

In summary, the TRPC-like Ca^{2+} entry mechanism in OHCs is a new element in hair cell Ca^{2+} signalling, which contributes to the regulation of sound transduction and auditory neurotransmission. The OHC TRPC conductance provides a negatively regulated feedback pathway for Ca^{2+} entry which contributes to Ca^{2+} homeostasis, and via activation by DAG, complements GPCR-mediated Ca^{2+} signalling. The TRPC Ca^{2+} entry current is closely linked to K_{Ca} channel activation and influences the OHC membrane conductance. The pharmacological and biophysical properties of the TRPC-like Ca^{2+} current are compatible with either homomeric or heteromeric TRPC ion channel assembly with TRPC3 subunits expressed by the hair cells.

References

Ashmore JF & Ohmori H (1990). Control of intracellular calcium by ATP in isolated outer hair cells of the guinea-pig cochlea. *J Physiol* **428**, 109–131.

Beurg M, Hafidi A, Skinner LJ, Ruel J, Nouvian R, Henaff M, Puel JL, Aran JM & Dulon D (2005). Ryanodine receptors and BK channels act as a presynaptic depressor of neurotransmission in cochlear inner hair cells. *Eur J Neurosci* **22**, 1109–1119.

Beutner D, Voets T, Neher E & Moser T (2001). Calcium dependence of exocytosis and endocytosis at the cochlear inner hair cell afferent synapse. *Neuron* **29**, 681–690.

Chan DK & Hudspeth AJ (2005). Ca^{2+} current-driven nonlinear amplification by the mammalian cochlea in vitro. *Nat Neurosci* **8**, 149–155.

Clapham DE (2003). TRP channels as cellular sensors. *Nature* **426**, 517–524.

Corey DP (2006). What is the hair cell transduction channel? *J Physiol* **576**, 23–28.

Corey DP, Garcia-Anoveros J, Holt JR, Kwan KY, Lin SY, Vollrath MA, Amalfitano A, Cheung EL, Derfler BH, Duggan A, Geleoc GS, Gray PA, Hoffman MP, Rehm HL, Tamasauskas D & Zhang DS (2004). TRPA1 is a candidate for the mechanosensitive transduction channel of vertebrate hair cells. *Nature* **432**, 723–730.

Dallos P, He DZ, Lin X, Sziklai I, Mehta S & Evans BN (1997). Acetylcholine, outer hair cell electromotility, and the cochlear amplifier. *J Neurosci* **17**, 2212–2226.

Dumont RA, Lins U, Filoteo AG, Penniston JT, Kachar B & Gillespie PG (2001). Plasma membrane Ca^{2+}-ATPase isoform 2a is the PMCA of hair bundles. *J Neurosci* **21**, 5066–5078.

Evans MG, Lagostena L, Darbon P & Mammano F (2000). Cholinergic control of membrane conductance and intracellular free Ca^{2+} in outer hair cells of the guinea pig cochlea. *Cell Calcium* **28**, 195–203.

Frolenkov GI, Mammano F, Belyantseva IA, Coling D & Kachar B (2000). Two distinct Ca^{2+}-dependent signaling pathways regulate the motor output of cochlear outer hair cells. *J Neurosci* **20**, 5940–5948.

Gamper N, Stockand JD & Shapiro MS (2003). Subunit-specific modulation of KCNQ potassium channels by Src tyrosine kinase. *J Neurosci* **23**, 84–95.

Hafidi A, Beurg M & Dulon D (2005). Localization and developmental expression of BK channels in mammalian cochlear hair cells. *Neuroscience* **130**, 475–484.

Hofmann T, Obukhov AG, Schaefer M, Harteneck C, Gudermann T & Schultz G (1999). Direct activation of human TRPC6 and TRPC3 channels by diacylglycerol. *Nature* **397**, 259–263.

Hofmann T, Schaefer M, Schultz G & Gudermann T (2002). Subunit composition of mammalian transient receptor potential channels in living cells. *Proc Natl Acad Sci U S A* **99**, 7461–7466.

Housley GD & Ashmore JF (1991). Direct measurement of the action of acetylcholine on isolated outer hair cells of the guinea pig cochlea. *Proc R Soc Lond B* **244**, 161–167.

Housley GD & Ashmore JF (1992). Ionic currents of outer hair cells isolated from the guinea-pig cochlea. *J Physiol* **448**, 73–98.

Housley GD, Connor BJ & Raybould NP (1995). Purinergic modulation of outer hair cell electromotility. In *Active Hearing*, 1st edn, ed. Flock Å, Ottoson D & Ulfendahl M, pp. 221–238. Pergamon, Oxford.

Housley GD, Kanjhan R, Raybould NP, Greenwood D, Salih SG, Järlebark L, Burton LD, Setz VC, Cannell MB, Soeller C, Christie DL, Usami S, Matsubara A, Yoshie H, Ryan AF & Thorne PR (1999). Expression of the $P2X_2$ receptor subunit of the ATP-gated ion channel in the cochlea: implications for sound transduction and auditory neurotransmission. *J Neurosci* **19**, 8377–8388.

Housley GD, Marcotti W, Navaratnam D & Yamoah E (2006). Hair cells – beyond the transducer. *J Memb Biol* **209**, 89–118.

Hu HZ, Gu Q, Wang C, Colton CK, Tang J, Kinoshita-Kawada M, Lee LY, Wood JD & Zhu MX (2004). 2-aminoethoxydiphenyl borate is a common activator of TRPV1, TRPV2, and TRPV3. *J Biol Chem* **279**, 35741–35748.

Kawasaki BT, Liao Y & Birnbaumer L (2006). Role of Src in C3 transient receptor potential channel function and evidence for a heterogeneous makeup of receptor-and store-operated Ca^{2+} entry channels. *Proc Natl Acad Sci U S A* **103**, 335–340.

Kennedy HJ, Crawford AC & Fettiplace R (2005). Force generation by mammalian hair bundles supports a role in cochlear amplification. *Nature* **433**, 880–883.

Kennedy HJ, Evans MG, Crawford AC & Fettiplace R (2003). Fast adaptation of mechanoelectrical transducer channels in mammalian cochlear hair cells. *Nat Neurosci* **6**, 832–836.

Khan KM, Drescher MJ, Hatfield JS, Khan AM & Drescher DG (2002). Muscarinic receptor subtypes are distributed in the rat cochlea. *Neuroscience* **111**, 291–302.

Kwan KY, Allchorne AJ, Vollrath MA, Christensen AP, Zhang D-S, Woolf CJ & Corey DP (2006). TRPA1 contributes to cold, mechanical and chemical nociception but is not essential for hair-cell transduction. *Neuron* **50**, 277–289.

Lemonnier L, Prevarskaya N, Mazurier J, Shuba Y & Skryma R (2004). 2-APB inhibits volume-regulated anion channels independently from intracellular calcium signaling modulation. *FEBS Lett* **556**, 121–126.

Liedtke W, Choe Y, Marti-Renom MA, Bell AM, Denis CS, Sali A, Hudspeth AJ, Friedman JM & Heller S (2000). Vanilloid receptor-related osmotically activated channel (VR-OAC), a candidate vertebrate osmoreceptor. *Cell* **103**, 525–535.

Lievremont JP, Bird GS & Putney JW Jr (2005). Mechanism of inhibition of TRPC cation channels by 2-aminoethoxydiphenylborane. *Mol Pharmacol* **68**, 758–762.

Lintschinger B, Balzer-Geldsetzer M, Baskaran T, Graier WF, Romanin C, Zhu MX & Groschner K (2000). Coassembly of Trp1 and Trp3 proteins generates diacylglycerol- and Ca^{2+}-sensitive cation channels. *J Biol Chem* **275**, 27799–27805.

Lioudyno M, Hiel H, Kong JH, Katz E, Waldman E, Parameshwaran-Iyer S, Glowatzki E & Fuchs PA (2004). A 'synaptoplasmic cistern' mediates rapid inhibition of cochlear hair cells. *J Neurosci* **24**, 11160–11164.

López-Candales A, Scott MJ & Wickline SA (1995). Cholesterol feeding modulates spatial expression of TGF-beta 1 and beta 2 in aortas of Watanabe rabbits. *Cytokine* **7**, 554–561.

Ma HT, Patterson RL, van Rossum DB, Birnbaumer L, Mikoshiba K & Gill DL (2000). Requirement of the inositol trisphosphate receptor for activation of store-operated Ca^{2+} channels. *Science* **287**, 1647–1651.

Mammano F & Ashmore JF (1996). Differential expression of outer hair cell potassium currents in the isolated cochlea of the guinea-pig. *J Physiol* **496**, 639–646.

Mammano F, Frolenkov GI, Lagostena L, Belyantseva IA, Kurc M, Dodane V, Colavita A & Kachar B (1999). ATP-Induced Ca^{2+} release in cochlear outer hair cells: localization of an inositol triphosphate-gated Ca^{2+} store to the base of the sensory hair bundle. *J Neurosci* **19**, 6918–6929.

Marcotti W & Kros CJ (1999). Developmental expression of the potassium current $I_{K,n}$ contributes to maturation of mouse outer hair cells. *J Physiol* **520**, 653–660.

Maruyama T, Kanaji T, Nakade S, Kanno T & Mikoshiba K (1997). 2APB, 2-aminoethoxydiphenyl borate, a membrane-penetrable modulator of Ins(1,4,5)P3-induced Ca^{2+} release. *J Biochem* **122**, 498–505.

Mizuno N, Kitayama S, Saishin Y, Shimada S, Morita K, Mitsuhata C, Kurihara H & Dohi T (1999). Molecular cloning and characterization of rat trp homologues from brain. *Brain Res Mol Brain Res* **64**, 41–51.

Mori Y, Takada N, Okada T, Wakamori M, Imoto K, Wanifuchi H, Oka H, Oba A, Ikenaka K & Kurosaki T (1998). Differential distribution of TRP Ca^{2+} channel isoforms in mouse brain. *Neuroreport* **9**, 507–515.

Nenov AP, Norris C & Bobbin RP (1997). Outwardly rectifying currents in guinea pig outer hair cells. *Hear Res* **105**, 146–158.

Okada T, Inoue R, Yamazaki K, Maeda A, Kurosaki T, Yamakuni T, Tanaka I, Shimizu S, Ikenaka K, Imoto K & Mori Y (1999). Molecular and functional characterization of a novel mouse transient receptor potential protein homologue TRP7. Ca^{2+}-permeable cation channel that is constitutively activated and enhanced by stimulation of G protein-coupled receptor. *J Biol Chem* **274**, 27359–27370.

Okamura H, Spicer SS & Schulte BA (2001). Immunohistochemical localization of phospholipase C isozymes in mature and developing gerbil cochlea. *Neuroscience* **102**, 451–459.

Oliver D, Klocker N, Schuck J, Baukrowitz T, Ruppersberg JP & Fakler B (2000). Gating of Ca^{2+}-activated K^{+} channels controls fast inhibitory synaptic transmission at auditory outer hair cells. *Neuron* **26**, 595–601.

Putney JW Jr (2004). The enigmatic TRPCs: multifunctional cation channels. *Trends Cell Biol* **14**, 282–286.

Ramsey IS, Delling M & Clapham DE (2006). An introduction to TRP channels. *Annu Rev Physiol* **68**, 619–647.

Raybould NP & Housley GD (1997). Variation in expression of the outer hair cell P2X receptor conductance along the guinea-pig cochlea. *J Physiol* **498**, 717–727.

Raybould NP, Jagger DJ & Housley GD (2001). Positional analysis of guinea pig inner hair cell membrane conductances: implications for regulation of the membrane filter. *J Assoc Res Otolaryngol* **2**, 362–376.

Shen J, Harada N, Kubo N, Liu B, Mizuno A, Suzuki M & Yamashita T (2006). Functional expression of transient receptor potential vanilloid 4 in the mouse cochlea. *Neuroreport* **17**, 135–139.

Soeller C & Cannell MB (1996). Construction of a two-photon microscope and optimisation of illumination pulse duration. *Pflugers Arch* **432**, 555–561.

Sridhar TS, Brown MC & Sewell WF (1997). Unique postsynaptic signaling at the hair cell efferent synapse permits calcium to evoke changes on two time scales. *J Neurosci* **17**, 428–437.

Strotmann R, Schultz G & Plant TD (2003). Ca^{2+}-dependent potentiation of the nonselective cation channel TRPV4 is mediated by a C-terminal calmodulin binding site. *J Biol Chem* **278**, 26541–26549.

Strubing C, Krapivinsky G, Krapivinsky L & Clapham DE (2001). TRPC1 and TRPC5 form a novel cation channel in mammalian brain. *Neuron* **29**, 645–655.

Tang J, Lin Y, Zhang Z, Tikunova S, Birnbaumer L & Zhu MX (2001). Identification of common binding sites for calmodulin and inositol 1,4,5-trisphosphate receptors on the carboxyl termini of trp channels. *J Biol Chem* **276**, 21303–21310.

Trebak M, Bird GS, McKay RR & Putney JW Jr (2002). Comparison of human TRPC3 channels in receptor-activated and store-operated modes. Differential sensitivity to channel blockers suggests fundamental differences in channel composition. *J Biol Chem* **277**, 21617–21623.

Vazquez G, Wedel BJ, Kawasaki BT, Bird GS & Putney JW Jr (2004). Obligatory role of Src kinase in the signaling mechanism for TRPC3 cation channels. *J Biol Chem* **279**, 40521–40528.

Yamamoto T, Kakehata S, Yamada T, Saito T, Saito H & Akaike N (1997). Effects of potassium channel blockers on the acetylcholine-induced currents in dissociated outer hair cells of guinea pig cochlea. *Neurosci Lett* **236**, 79–82.

Zhang Z, Tang J, Tikunova S, Johnson JD, Chen Z, Qin N, Dietrich A, Stefani E, Birnbaumer L & Zhu MX (2001). Activation of Trp3 by inositol 1,4,5-trisphosphate receptors through displacement of inhibitory calmodulin from a common binding domain. *Proc Natl Acad Sci U S A* **98**, 3168–3173.

Zheng J, Shen W, He DZ, Long KB, Madison LD & Dallos P (2000). Prestin is the motor protein of cochlear outer hair cells. *Nature* **405**, 149–155.

Zitt C, Halaszovich CR & Luckhoff A (2002). The TRP family of cation channels: probing and advancing the concepts on receptor-activated calcium entry. *Prog Neurobiol* **66**, 243–264.

Zucchi R & Ronca-Testoni S (1997). The sarcoplasmic reticulum Ca^{2+} channel/ryanodine receptor: modulation by endogenous effectors, drugs and disease states. *Pharmacol Rev* **49**, 1–51.

Acknowledgements

The authors thank Jacqui Ross of the Biomedical Imaging Unit and Angus McMorland for assistance. The study was funded by: Health Research Council (NZ); James Cook Fellowship (Royal Society NZ) (GDH), Marsden Fund (Royal Society NZ); Auckland Medical Research Foundation.